

# On the Nature of the Rapidity-Spectra at RHIC and Some Other Energies.

Goutam Sau<sup>1,\*</sup>, S. K. Biswas<sup>2,†</sup>, A. C. Das Ghosh<sup>3,‡</sup>, A. Bhattacharya<sup>4,§</sup> & S. Bhattacharyya<sup>5,¶</sup>

<sup>1</sup> Beramara RamChandrapur High School,  
South 24-Pgs, 743609(WB), India.

<sup>2</sup> West Kodalia Adarsha Siksha Sadan,  
New Barrackpore, Kolkata-700131, India.

<sup>3</sup> Department of Microbiology,  
Surendranath College, Kolkata-700009, India.

<sup>4</sup> Department of Physics,  
Jadavpur University, Kolkata- 700032, India.

<sup>5</sup> Physics and Applied Mathematics Unit(PAMU),  
Indian Statistical Institute, Kolkata - 700108, India.

## Abstract

On the basis of the Grand Combinational Model (GCM) outlined and somewhat detailed in the text, we have attempted to capture here the several interesting assorted characteristics of the rapidity-spectra of the major varieties of secondaries produced in diverse nuclear reactions at various energies, though the main thrust of our work lies on addressing the data-trends from RHIC-BNL experiments. Obviously the core of the present approach is purely phenomenological. Still, the method and the model address the features of the data modestly well. And the method appears to have the rich potentiality, if the systematic sets of data for rapidity-studies at gradually increasing energies were available.

Keywords: Relativistic heavy ion collisions; inclusive cross-section.

PACS nos.: 25.75.-q, 13.60.Hb

---

\*e-mail: sau\_goutam@yahoo.com

†e-mail: sunil\_biswas2004@yahoo.com

‡e-mail: dasghosh@yahoo.co.in

§e-mail: pampa@phys.jdvu.ac.in

¶e-mail: bsubrata@www.isical.ac.in (Communicating Author).

# 1 Introduction

Unlike the cases of  $p_T$ -spectra, theoretical (even phenomenological), studies on the rapidity-spectra are relatively much fewer, though these two observables  $[(p_T, y)$  or  $(p_T, \eta)]$  are just twins for analyzing the nature of invariant cross-sections for the secondary particles produced in the arranged laboratory collisions at very high energies. In fact, the experimentalists also are not immune from such biases, mainly due to the accompanying difficulties in the measurement processes. And the net effect of all these put together is the number of data sets on rapidity spectra is obviously much less abundant and they suffer from large measuremental uncertainties or large errors of both systematic and statistical nature. Despite these strong and somewhat insurmountable limitations, in the present work we will confine ourselves to the studies on rapidity-spectra produced in Pb+Pb reactions at marginally high energies and in RHIC-BNL interactions involving Au+Au collisions at  $\sqrt{s_{NN}} = 200$  GeV in the light of Grand Combinational Model (GCM). The stimulus stems from the fact that in the past we analyzed a large part of the data on  $p_T$ -spectra for RHIC-BNL collisions and a considerable part of the rapidity-spectra at CERN SPS-energies. So, for the sake of completeness of our studies on the behaviour of this specific model (GCM), we need to check whether this model as such (or any extension of the model for higher energies) could explain the relatively sparse data on the rapidity-spectra and some other related properties involving these experimental measurements on rapidity-dependent physical observables.

The plan of this paper is as follows. In Section 2, we attempt to provide an outline of the Grand Combinational Method (GCM) and give the successive procedural steps. The Section 3 gives an inkling into the basic root of the expressions used in Section 2. The Section 4 exhibits the results and some discussions on them. The last Section (Section 4) contains the final summary and the conclusive remarks.

# 2 The Working Model : An Outlook

Following Faessler[1], Peitzmann[2] and also the work of Schmidt and Schukraft[3], we propose here a generalized empirical relationship between the inclusive cross-section for production of any particle represented by  $Q$  in nucleus-nucleus collision and production of the same in nucleon-nucleon

collisions in the following form :

$$E \frac{d^3\sigma}{dp^3}|_{AB \rightarrow QX} \sim (AB)^{\epsilon(y,p_T)} E \frac{d^3\sigma}{dp^3}|_{PP \rightarrow QX}, \quad (1)$$

where  $Q$  is the secondary, like pion/kaon/proton/antiproton, produced in high energy nucleus-nucleus(AB) or in proton-proton(PP) collisions. The term  $\epsilon(y, p_T)$  could be expressed in the factorization form  $\epsilon(y, p_T) = f(y)g(p_T)$ . While investigating a specific nature of dependence of the two variables ( $y$  and  $p_T$ ), either of them is assumed to remain averaged or with definite values. Speaking in clearer terms, if and when rapidity dependence is studied by experimental group, the transverse momentum is integrated over certain limits and is absorbed in the normalization factor. So the effective formula for rapidity spectra turns into

$$\frac{d\sigma}{dy}|_{AB \rightarrow QX} \sim (AB)^{f(y)} \frac{d\sigma}{dy}|_{PP \rightarrow QX}. \quad (2)$$

The main bulk of work, thus, converges to the making of an appropriate choice of form for  $f(y)$ . And the necessary choice is to be made on the basis of certain premises and physical considerations which do not violate the canons of high energy interactions.

Applying the concept of both limiting fragmentation and the Feynman Scaling hypothesis we attempt at providing first a fit to the data on rapidity distributions for proton-proton collisions at several  $\sqrt{s}$  values, ranging from  $\sqrt{s} = 23$  GeV to 63 GeV with a parametrization by 3-parameter formula :

$$\frac{1}{\sigma} \frac{d\sigma}{dy} = C_1 (1 + \exp \frac{y - y_0}{\Delta})^{-1} \quad (3)$$

where  $C_1$  is a normalization constant and  $y_0$ ,  $\Delta$  are two parameters. The choice of the above form made by Thome' et al[4] was intended to describe conveniently the central plateau and the fall-off in the fragmentation region by means of the parameters  $y_0$  and  $\Delta$  respectively. For all five energies in PP collisions the value of  $\Delta$  was obtained to be  $\sim 0.55$  for pions[5] and kaons[6], and  $\sim 0.35$  for protons/antiprotons[6]. And these values of  $\Delta$  are generally assumed to remain the same in the ISR ranges of energy. Still, for very high energies, and for direct fragmentation processes which are quite feasible in very high energy heavy nucleus-nucleus collisions, such parameter values do change somewhat prominently, though in most cases with marginal high energies, we have treated them as nearly constant.

Now, the fits for the rapidity (pseudorapidity) spectra for non-pion secondaries produced in the PP reactions at various energies are phenomenologically obtained by De and Bhattacharyya[6]

through the making of suitable choices of  $C_1$  and  $y_0$ . It is observed that for various secondaries the values of  $y_0$  remain almost constant and do not show up any sharp species-dependence amongst the secondaries. However, for pions it gradually increases with energies and the energy-dependence of  $y_0$  is empirically proposed to be expressed by the relationship[5] :

$$y_0 = 0.55 \ln \sqrt{s_{NN}} + 0.88 \quad (4)$$

However, the energy-dependence of  $y_0$  is studied here just for gaining insights in their nature and for purposes of extrapolation to the various higher energies (in the frame of  $\sqrt{s_{NN}}$ ) for several nucleon-nucleus and nucleus-nucleus collisions. The specific energy (in the c.m. system,  $\sqrt{s_{NN}}$ ) for every nucleon-nucleus or nucleus-nucleus collision is first worked out by converting the laboratory energy value(s) in the required c.m. frame energy value(s). Thereafter the value of  $y_0$  to be used for computations of inclusive cross-sections of nucleon-nucleon collisions at particular energies of interactions is extracted from Eq. (4) for corresponding obtained energies. This procedural step is followed for calculating the rapidity (pseudorapidity)-spectra for only the pions produced in nucleon-nucleus and nucleus-nucleus collisions[5]. But, for the studies on the rapidity-spectra of the non-pion secondaries produced in the same reactions one does neither have the opportunity to take recourse to such systematic step, nor could they actually resort to this rigorous procedure, as both the values of  $y_0$  and  $\Delta$  (as was done by De and Bhattacharyya[6]) do not depict any sensitive energy-dependences. So, we have considered only the average values of  $y_0$  and  $\Delta$  to study the rapidity spectra for non-pion secondaries produced in nucleon (nucleus)-nucleus collisions.

Our next step is to explore the nature of  $f(y)$  which is envisaged to be given generally by a polynomial form noted below :

$$f(y) = \alpha + \beta y + \gamma y^2, \quad (5)$$

where  $\alpha$ ,  $\beta$  and  $\gamma$  are the coefficients to be chosen separately for each AB collisions (and also for AA collisions when the projectile and the target are same). But, in so far as dealing with the rapidity spectra is concerned, the above expression suffers from a limitation which we would discuss later in some detail in section 3.2. Besides, some other points are to be made here. The suggested choice of form in expression (5) is not altogether fortuitous. In fact, we got the clue from one of the previous work by one of the authors (SB)[7] here pertaining to the studies on the behavior of the EMC effect related to the lepto-nuclear collisions. In the recent past Hwa et al[8] also made use of this sort of relation in a somewhat different context. Now we go back to our original discussion.

Combining Eqs. (2) and (5) the final working formula for  $\frac{dN}{dy}$  in various AB (or AA) collisions can be expressed by the following relation :

$$\frac{dN}{dy}|_{AB \rightarrow QX} = C_2(AB)^{\alpha+\beta y+\gamma y^2} \frac{dN}{dy}|_{PP \rightarrow QX} = C_3(AB)^{\beta y+\gamma y^2} (1 + \exp \frac{y-y_0}{\Delta})^{-1}, \quad (6)$$

where  $C_2$  is the normalization constant and  $C_3=C_2(AB)^\alpha$  is another constant as  $\alpha$  is also a constant for a specific collision at a specific energy. The parameter values for different nucleus-nucleus collisions are given in Table1 - Table 9. However, in the next section (Section 3) we attempt at providing hints to the possible origin of our very starting equation [Eqn. 1] in this Section.

### 3 Basic Sources of the Theoretical Framework : An Outline

At the very root, our approach owes a lot to the basics of the Glauber Model and to the pioneering developmental works by Gribov who showed how to incorporate the Glauber Model for interactions of hadrons with nuclei into the general framework of relativistic quantum theory. Subsequently, an important contribution to the theory multiparticle production was made by Gribov jointly with Abramovsky and Kancheli which is normally referred to as the AGK cutting rules. Later Capella et al[16] combined in an excellent work the outcomes of all of them in a concise paper from which we pick up the expressions having very close resemblance with both the physical ideas, the terms and also the mathematical structure.

An important consequence of the space-time structure of the scattering diagrams for hadron-nucleus interactions as studied by Capella et al is : for inclusive cross sections all rescatterings cancel with each other and the cross sections are determined solely by the very common impulse approximation. This statement is valid asymptotically in the central rapidity region ( $y \simeq 0$ ) and for cases where the masses of the intermediate studies are both limited and energy-independent.

The inclusive cross section for the production of a hadron  $i$  is expressed, for a given impact parameter  $b$ , in terms of inclusive cross section for hN interactions[12]

$$E \frac{d^3 \sigma_{hA}^i(b)}{d^3 p} = T_A(b) E \frac{d^3 \sigma_{hN}^i}{d^3 p} \quad (7)$$

where  $T_A(b)$  is the nuclear profile function ( $\int d^2 b T_A(b) = A$ ). After integrating over  $b$  we get

$$E \frac{d^3 \sigma_{hA}^i}{d^3 p} = A E \frac{d^3 \sigma_{hN}^i}{d^3 p} \quad (8)$$

The total and inelastic hA cross sections in the Glauber model can be easily calculated and are given for heavy nuclei by well known expressions. For example

$$\sigma_{hA}^{in} = \int d^2b (1 - \exp(-\sigma_{hN}^{in} T_A(b))) \quad (9)$$

The situation for nucleus-nucleus collisions is much more complicated. There are no analytic expressions in the Glauber model for heavy-nuclei elastic scattering amplitudes. The problem stems from a complicated combinatorics and from the existence of dynamical correlations related to “loop diagrams” [13, 14]. Thus, usually optical-type approximation [15, 16] and probabilistic models for multiple rescatterings [17] are used. For inclusive cross sections in AB-collisions the result of the Glauber approximation is very simple to formulate due to the AGK cancelation theorem. It is possible to prove, for an arbitrary number of interactions of nucleons of both nuclei [18], that all rescatterings cancel in the same way as for hA-interactions. Thus a natural generalization of eq. (7) for inclusive spectra of hadrons produced in the central rapidity region in nucleus-nucleus interactions takes place in the Glauber approximation

$$E \frac{d^3 \sigma_{AB}^i(b)}{d^3 p} = T_{AB}(b) E \frac{d^3 \sigma_{NN}^i}{d^3 p} \quad (10)$$

where  $T_{AB}(b) = \int d^2s T_A(\vec{s}) T_B(\vec{b} - \vec{s})$ . After integration over  $b$  eq. (10) reads

$$E \frac{d^3 \sigma_{AB}^i}{d^3 p} = AB E \frac{d^3 \sigma_{NN}^i}{d^3 p} \quad (11)$$

It is to be noted here that eqs. (10), (11) are valid for an arbitrary set of Glauber diagrams and are not influenced by the problem of summation of “loop” diagrams mentioned above.

The densities of charged particles can be obtained from eqs. (10), (11) by dividing them by the total inelastic cross section of nucleus-nucleus interaction. For example

$$\frac{dn_{AB}^{ch}(b)}{dy} = \frac{T_{AB}(b)}{\sigma_{AB}^{in}} \frac{d\sigma_{NN}^{ch}}{dy} \quad (12)$$

and

$$\frac{dn_{AB}^{ch}}{dy} = \frac{AB}{\sigma_{AB}^{in}} \frac{d\sigma_{NN}^{ch}}{dy} \quad (13)$$

In the following we shall use these results to calculate particle densities in the central rapidity region at energies of RHIC and LHC. It is to be seen that our starting expression [eqn. (1)] is just a generalization of the expression (11) shown here.

## 4 Results

This section is to be divided into three Subsections. In the first one we summarize the procedural steps that follow from the Section-2. And in the rest the results are delivered.

### 4.1

The procedural steps for arriving at the results could be summed up as follows :

(i) We assume that the inclusive cross section (I.C.) of any particle in a nucleus-nucleus (AB) collision can be obtained from the production of the same in nucleon-nucleon collisions by multiplying it (I.C.) a product of the atomic numbers of each of the colliding nuclei raised to a particular function,  $\epsilon(y, p_T)$ , which at first is unspecified (Equation 1).

(ii) Secondly, we accept that factorization of the function  $\epsilon(y, p_T) = f(y)g(p_T)$  which helps us to perform the integral over  $p_T$  (Equation 2) in a relatively simpler manner.

(iii) Thirdly, we assume a particular 3-parameter form for the pp cross section with the parameters  $C_1$ ,  $y_0$  and  $\Delta$  (Equation 3).

(iv) Finally, we accept the ansatz that the function  $f(y)$  can be modeled by a quadratic function with the parameters  $\alpha$ ,  $\beta$  and  $\gamma$  (Equation 5).

### 4.2

The results are shown here by the graphical plots with the accompanying tables for the parameter values. In Fig.1 we draw the rapidity-density of the negative pions for symmetric Pb+Pb collisions at several energies which have been appropriately labeled at the top-right corner. In this context some comments are in order. Though the figure represents the case for production of negative pions, we do not anticipate and/or expect any strong charge-dependence of the results. Besides, the **solid** curves in all cases - almost without any exception - demonstrate our GCM-based results. Secondly, the data on rapidity-spectra for some high-energy collisions are, at times, available for both positive and negative  $y$ -values. This gives rise to a problem in our method. It is evident here in this work that we are concerned with only symmetric collisions wherein the colliding nuclei must be identical. But in our expression (6) the coefficient  $\beta$  multiplies a term which is proportional to  $y$  and so is **not** symmetric under  $y \rightarrow (-y)$ . In order to overcome this difficulty we would introduce here  $\beta=0$  for a large number of the graphical plots. These plots are represented by Fig.1, Fig.2,

Fig.5, Fig.6 and Fig.7 for the various secondaries produced in Au+Au/Pb+Pb collisions under different conditions of relatively low c.m. energy values. The parameter values in this particular case are presented in the Tables 1,2,3,6,7,8,9. The Fig.2a and 2b (both for  $\beta=0$ ) are for production of positive kaon and negative kaons in Pb+Pb interactions at 30A GeV and 20A GeV. But the Fig.3 is based on the data on pion-production in Au+Au collisions at several relatively low energies for which data are available on  $dn/dy$  (rapidity density of multiplicity) versus only positive  $y$ -values. The parameter values are presented in Table4. And the diagrams in Fig.4 represent the production of the major varieties of the secondaries produced in Au+Au collisions at RHIC; herein too the data are obtained for only positive values of rapidity. The corresponding parameter values are presented in Table5.

### 4.3

But the problem starts as soon as we attempt to reproduce the trends in data simultaneously for both +ve and -ve rapidity values. The graphs grow asymmetric even for symmetric collision. In Fig.5 with  $K^\pm$ -meson varieties we tried to fix and focus the problem encountered. The four labeled diagrams for  $K^\pm$ -meson varieties shown in the present Fig.5 provide fits to the data with unchanged  $\Delta$ -values ( $\Delta=0.55$ ) for both positive and negative  $y$ -values quite separately. The parameter values are to be obtained from Table6 and Table7. These plots provide very important clues to our understanding the nature of  $\Delta$ -values at very, very high energies. For both kaon-antikaons one observes quite clearly that the plots end up on the X-(rapidity)-axis for positive high- $y$ -values within the range +5 to +6 (positive)  $y$ -values, whereas for the **negative** high  $y$ -values the spread widens to  $y$ -values ranging between -6 to -7. This shows up somewhat convincingly to us that the asymmetry problem arising in Fig.5 towards the +ve  $y$ -values cannot be addressed properly and remedied without inserting necessary changes in the accompanying sets of parameters, as the treated energy-ranges for these Au+Au collision cases are very high compared to the various sets of other data presented here. Our studied diagnosis of the root of the problem forced us to alter the previous  $\Delta$ -values with phenomenological induction of increasing the nature of  $\Delta$  with rising energy as was the case for  $y_0$ . And, thus, making use of this ansatz, we were able to redeem the symmetry-feature of the rapidity plots. The subsequent two figures, the Fig.6 and Fig.7 strikingly illustrate how the qualitative improvement in the nature of the plots on rapidity-distributions for Au+Au reaction at RHIC was achieved by changing  $\Delta$ -values. The parameter values for Fig.6 and



Fig.7 are given in Table8 and Table9. The Fig.6 and Fig.7 (for  $\beta=0$ ) describe the rapidity spectra on the various non-pion secondaries as labeled in Figs. 6(a), 6(b), 6(c), 6(d) and Figs. 7(a), 7(b), 7(c), 7(d) for both positive and negative y-values in Au+Au collisions at RHIC energies with  $\Delta$ -value=1.70 and  $\Delta$ -value=3.5 respectively. Due to the paucity of data, we are not going to present, at this juncture, any quantitative prediction on the nature of rise of  $\Delta$ , though we qualitatively accept and use it in this work.

#### 4.4

The diagrams shown in Fig.8(a) and Fig.8(b) represent the model-based results on  $K^+/\pi^+$  and  $K^-/\pi^-$  respectively. These plots are drawn on the basis of the figures shown in Fig.4 with the fit-parameters given in Table5. The data-trends have been captured by them in a modestly right manner. The next plot (Fig.9) pertains to the particle/antiparticle ratio-values which are really quite crucial. This plot is drawn with the help of the figures shown in Fig.4 and the Table5, that is, they were worked out on the basis of the graphs drawn in Fig.4 and the accompanying table displayed in the Table5.

The rest two plots, Fig.10(a) and Fig.10(b), are drawn on the basis of these revised figures with the gradually changed values of  $\Delta$ . As no data on a charge-dependent basis for pions produced in Au+Au reactions at RHIC energies with negative y-values were available, we could not depict the  $\pi^-/\pi^+$  ratio-behaviour in Fig.10(a) and Fig.10(b) with changed  $\Delta$ -values. And the physical justifications for introduction of such enhancements in the values of  $\Delta$  had already been hinted at quite emphatically in Section 2. They also reproduce the features of the data, in a fairly satisfactory manner. In fact, with changed  $\Delta$ -values they describe, in our opinion, data-characteristics in a somewhat better way.

## 5 Discussion and Conclusions

Surveying the model-based plots and judging by the degree and nature of agreement between the measured data and the obtained results, we could fairly sum up by a reasonable statement that the model(s) applied here describe the data in a modestly satisfactory manner. The used models have both a deductive origin and some phenomenological components, with some conceptual physical strands : (i) the results for the nucleus-nucleus collisions could be arrived at by inducting the results

of nucleon-nucleon collisions and some relevant phenomenological product terms incorporating the physics of nuclear dependences; (ii) the property of factorization is also embedded in the results in an ingrained manner; (iii) there is a certain degree of universality of nature among the secondaries produced in nucleon-nucleon, nucleon-nucleus and nucleus-nucleus interactions at high energies, by virtue of which the entire ranges of rapidity-spectra have here been analyzed with the help of two parameters ( $y_0$  and  $\Delta$ ) for PP collisions, and two other ( $\beta$  and  $y$ ) parameters for nucleus-nucleus collisions. Of them,  $y_0$  for pion-production cases alone could be obtained by a formula [eqn.(4)] suggested by us. Similar behaviours of  $y_0$  and  $\Delta$  are perfectly possible at very very high energies for all non-pion secondaries as well, though, in most cases, we leave them practically unchanged. However, There are some exceptions for Fig.6 and Fig.7. Thus, we are left with only two arbitrary parameters, which one should try to relate with the physics of nuclear geometry and collision dynamics. But there are some problems with the studies of the rapidity-spectra : firstly, the systematic studies on the rapidity spectra - both experimental and theoretical/phenomenological - are comparatively quite fewer in number ; secondly, the measurements suffer relatively from a higher degree of uncertainty. In fact, the centrality-dependent studies on rapidity spectra are not yet available, for which the studies on the relationship between nuclear geometry and the rapidity-spectra cannot yet be taken up either by us or others. Viewed from the angle of these existing limitations and constraints, we could humbly claim that the task of explaining the data-trends and behaviours on rapidity spectra is done here with a modest degree of success. We have checked that with the changed values of  $\Delta$ , it is easier to describe the totality of data assembled here on several symmetric collisions at various energies within the domain of high energy ranges.

In our work, we have categorically pointed out the problem of treating the cases of negative rapidity-values with the help of the generalized expression given by expression (6), wherein a specific term as is indicated clearly in 4.2 constitutes the limitation of the method. For some other similar cases, however, the method remains fully valid and works phenomenologically quite well.

There is yet another drawback of this model. Since the coefficients are fit for different species and collision energies we cannot right now extrapolate to different collision energies or connect the various coefficients, nor could we make a reliable prediction for Pb+Pb collision at LHC on the basis of our fits to the RHIC data for Au+Au collisions. As a result, the model lacks, so far, any strong predictive power. And this is true of almost any phenomenological model whatsoever. But this difficulty could be remedied to a considerable extent, had there been availability of reliable and

accurate data at different high energies with reasonably spaced intervals for both PP interactions and/or any other symmetric high energy nuclear collisions. Besides, we are yet to find and work out the ways and means for adaptation of this methodology to any non-symmetric collision.

### **Acknowledgements**

The authors express their thankful gratitude to the learned Referee for some inspiring comments and constructive queries-cum-suggestions for improving the quality of an earlier version of the manuscript.

## References

- [1] M.A.Faessler : Phys. Rep. **115**, 1 (1984).
- [2] T.Peitzmann : Phys. Lett. **B 450**, 7 (1999).
- [3] H.R.Schmidt and J.Schukraft : J. Phys. **G 19**, 1705 (1993).
- [4] W.Thome' et al : Nucl. Phys. **B 129**, 365 (1977).
- [5] B.De, S.Bhattacharyya and P.Guptaroy : Int. J. Mod. Phys. **A 17**, 4615 (2002).
- [6] B.De and S.Bhattacharyya : Int. J. Mod.Phys. **A 19**, 2313 (2004).
- [7] S.Bhattacharyya : Lett. Nuovo Cimento **44**, 119 (1985).
- [8] R.C.Hwa et al : Phys. Rev. **C 64**, 054611 (2001).
- [9] R.J.Glauber : Lectures in Theoretical Physics. Ed. Britten W.E. N.Y. : Int. Publ. v.1, 315 (1959).
- [10] V.N.Gribov : JETP **56**, 892 (1969),  
V.N.Gribov : JETP **57**, 1306 (1969).
- [11] V.A.Abramovsky, V.N.Gribov and O.V.Kancheli : Sov. J. Nucl. Phys. **18**, 308 (1974).
- [12] A.Capella, A.Kaidalov and J.Tran Thanh Van : hep-ph/9903244 v1 03 March 1999; Contributed Paper to Gribov Memorial Volume of Acta Physica Hungarica (Heavy Ion Physics); Heavy Ion Phys. **9**, 169 (1999).
- [13] I.V. Andreev, A.V. Chernov : Yad. Fiz. **28**, 477 (1978).
- [14] K.G. Boreskov, A.B. Kaidalov : Yad. Fiz. **28**, 575 (1988).
- [15] J. Formanek : Nucl. Phys. **B 12**, 441 (1969).
- [16] W. Czyz and L.C. Maximon : Ann. Phys. (N.Y.) **52**, 59 (1969).
- [17] C. Pajares and A.V. Ramallo : Phys. Rev. **D 31**, 2800 (1985).
- [18] K.G. Boreskov, A.B. Kaidalov : Acta Phys. Polon. **B 20**, 397 (1989).
- [19] M.Mitrovski, T.Schuster, G.Gräf, H.Petersen, M.Bleicher : Phys. Rev. **C 79**, 044901 (2009) [ hep-ph/0812.2041 v1 10 December 2008 ].
- [20] C.Alt et al(NA49 collaboration) : Phys. Rev. **C 77**, 024903 (2008) [ nucl-ex/0710.0118 v1 30 September 2007 ].
- [21] Cheuk-Yin Wong : Phys. Rev. **C 78**, 054902 (2008) [ hep-ph/0808.1294 v1 08 August 2008 ].
- [22] Jun Song, Feng-lan Shao, Qu-bing Xie, Yun-fei Wang, De-ming Wei : Chinese Physics **C 33**, 481 (2009) [ nucl-th/0703095 v3 18 March 2008 ].

- [23] Saeed Uddin, Majhar Ali, Jan Shabir, M.Farooq Mir : hep-ph/0911.0246 v1 Submitted on 02 November 2009.
- [24] Saeed Uddin, Majhar Ali, Jan Shabir, M.Farooq Mir : hep-ph/0901.1376 v1 Submitted on 11 January 2009.
- [25] I.G.Bearden et al(BRAHMS Collaboration) : Phys. Rev. Lett. **94**, 162301 (2005) [ nucl-ex/0403050 v2 27 October 2004 ].

Table 1: Values of different parameters for production of negative-pions in Pb+Pb collisions at different energies(for  $\beta = 0$ ) for both +ve and -ve rapidities.[Reference Fig. No.1]

<i>Energy(GeV)</i>	$C_3$	$\gamma$	$\frac{\chi^2}{ndf}$
6.3	$87.426 \pm 0.403$	$-0.042 \pm 0.0006$	11.449/13
7.6	$100.095 \pm 0.291$	$-0.036 \pm 0.0003$	10.810/11
8.7	$118.278 \pm 0.274$	$-0.036 \pm 0.0002$	2.943/5
12.3	$147.107 \pm 0.401$	$-0.026 \pm 0.0002$	10.218/6
17.3	$184.850 \pm 0.449$	$-0.023 \pm 0.0001$	3.637/4

Table 2: Values of different parameters for production of kaons in Pb+Pb collisions at different energies for both +ve and -ve rapidities (for  $\beta=0$ ).[Reference Fig. No.2(a)]

<i>Energy</i>	$C_3$	$\gamma$	$\frac{\chi^2}{ndf}$
20AGeV	$5.798 \pm 0.015$	$-0.0903 \pm 0.0006$	0.673/3
30AGeV	$8.000 \pm 0.027$	$-0.0726 \pm 0.0005$	4.225/5

Table 3: Values of different parameters for production of anti-kaons in Pb+Pb collisions at different energies for both +ve and -ve rapidities (for  $\beta=0$ ).[Reference Fig. No.2(b)]

<i>Energy</i>	$C_3$	$\gamma$	$\frac{\chi^2}{ndf}$
20AGeV	$16.990 \pm 0.059$	$-0.0430 \pm 0.0020$	6.888/8
30AGeV	$21.589 \pm 0.066$	$-0.0404 \pm 0.0015$	7.282/11

Table 4: Values of different parameters for production of negative-pions in Au+Au collisions at different energies for +ve rapidities alone (for  $\beta \neq 0$ ).[Reference Fig. No.3]

<i>Energy(GeV)</i>	$C_3$	$\beta$	$\gamma$	$\frac{\chi^2}{ndf}$
8.8	$110.243 \pm 0.184$	$0.013 \pm 0.0002$	$-0.032 \pm 0.0002$	2.676/11
12.4	$147.023 \pm 0.369$	$0.005 \pm 0.0002$	$-0.019 \pm 0.0001$	6.494/9
17.3	$185.589 \pm 0.252$	$-0.006 \pm 0.0001$	$-0.009 \pm 0.0008$	3.238/8

Table 5: Values of the different parameters for production of pions, kaons, proton-antiprotons in Au+Au collisions at  $\sqrt{S_{NN}} = 200\text{GeV}$  for +ve rapidities alone (for  $\beta \neq 0$ ).[Reference Fig. No.4]

<i>Production</i>	$C_3$	$\beta$	$\gamma$	$\frac{\chi^2}{ndf}$
$\pi^+$	$303.480 \pm 0.400$	$0.0009 \pm 0.00007$	$0.0052 \pm 0.00002$	0.301/4
$\pi^-$	$300.938 \pm 1.981$	$0.0009 \pm 0.0003$	$0.0057 \pm 0.0001$	4.668/4
$K^+$	$49.169 \pm 0.099$	$0.0011 \pm 0.00009$	$0.0049 \pm 0.00003$	0.073/4
$K^-$	$46.996 \pm 0.073$	$0.0010 \pm 0.00009$	$0.0027 \pm 0.00003$	0.026/3
$P$	$24.862 \pm 0.659$	$0.009 \pm 0.002$	$0.0059 \pm 0.001$	3.431/8
$\bar{P}$	$17.794 \pm 0.290$	$0.011 \pm 0.003$	$-0.0059 \pm 0.001$	0.667/6

Table 6: Values of different parameters for production of kaon and antikaon in Au+Au collisions at  $\sqrt{S_{NN}} = 200\text{GeV}$  (for  $\beta = 0$ ) for +ve rapidity only, taking  $\Delta=0.55$ . [Reference Fig. No.5]

<i>Production</i>	$C_3$	$\gamma$	$\frac{\chi^2}{ndf}$
<i>Kaon</i>	$47.128 \pm 0.051$	$-0.005 \pm 0.0001$	1.941/09
<i>Anti - kaon</i>	$45.207 \pm 0.064$	$-0.008 \pm 0.0001$	1.018/06

Table 7: Values of different parameters for production of kaon and antikaon in Au+Au collisions at  $\sqrt{S_{NN}} = 200\text{GeV}$  (for  $\beta = 0$ ) for -ve rapidity only, taking  $\Delta=0.55$ . [Reference Fig. No.5]

<i>Production</i>	$C_3$	$\gamma$	$\frac{\chi^2}{ndf}$
<i>Kaon</i>	$47.808 \pm 0.076$	$-0.008 \pm 0.0001$	1.990/09
<i>Anti - kaon</i>	$46.705 \pm 0.069$	$-0.011 \pm 0.0001$	3.461/08

Table 8: Values of different parameters for production of proton, antiproton, kaon and antikaon in Au+Au collisions at  $\sqrt{S_{NN}} = 200\text{GeV}$  (for  $\beta = 0$ ) for both +ve and -ve rapidities, taking  $\Delta=1.7$ . [Reference Fig. No.6]

<i>Production</i>	$C_3$	$\gamma$	$\frac{\chi^2}{ndf}$
<i>Proton</i>	$49.770 \pm 0.690$	$-0.011 \pm 0.002$	2.083/09
<i>Anti - proton</i>	$21.103 \pm 0.408$	$-0.016 \pm 0.001$	4.636/13
<i>Kaon</i>	$55.524 \pm 0.111$	$-0.009 \pm 0.0003$	2.867/04
<i>Anti - kaon</i>	$48.660 \pm 0.109$	$-0.010 \pm 0.0003$	3.859/05

Table 9: Values of different parameters for production of proton, antiproton, kaon and antikaon in Au+Au collisions at  $\sqrt{S_{NN}} = 200\text{GeV}$  (for  $\beta = 0$ ) for both +ve and -ve rapidities, taking  $\Delta=3.5$ . [Reference Fig. No.7]

<i>Production</i>	$C_3$	$\gamma$	$\frac{\chi^2}{ndf}$
<i>Proton</i>	$59.529 \pm 1.028$	$-0.009 \pm 0.001$	4.924/13
<i>Anti - proton</i>	$25.107 \pm 0.469$	$-0.016 \pm 0.001$	5.160/13
<i>Kaon</i>	$67.962 \pm 0.228$	$-0.011 \pm 0.0003$	18.708/09
<i>Anti - kaon</i>	$66.694 \pm 0.198$	$-0.013 \pm 0.0003$	9.524/05

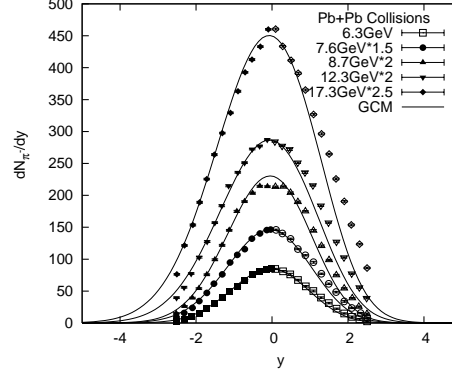


Figure 1: Rapidity spectra for secondary pions produced in Pb+Pb interactions at different energies for  $\beta = 0$ . The different experimental points are from Ref.[19] and the parameter values are taken from Table1. The solid curves provide the GCM-based results.

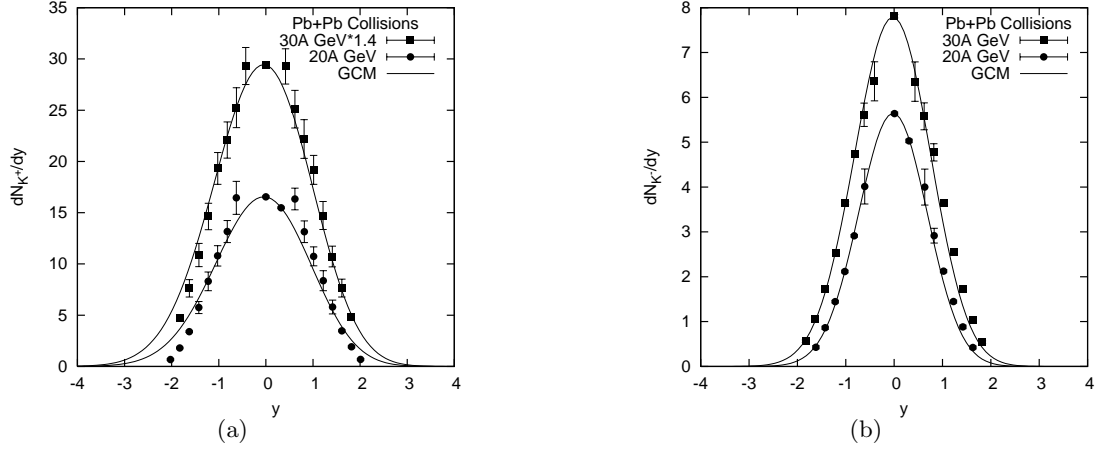


Figure 2: Rapidity distributions of  $K^+$  and  $K^-$  produced in central Pb+Pb collisions at 20A and 30A GeV(both for  $\beta = 0$ ). The different experimental points are from Ref.[20] and the parameter values are taken from Table2 and Table3. The solid curves provide the GCM-based results.



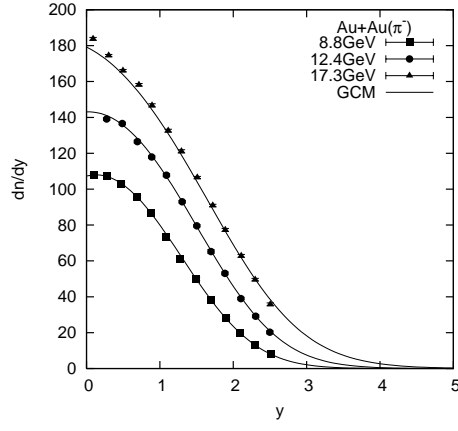


Figure 3: Rapidity spectra for negative secondary pions produced in Au+Au interactions at different energies (for  $\beta \neq 0$ ). The different experimental points are from Ref.[21] and the parameter values are taken from Table4. The solid curves show the GCM-based results.

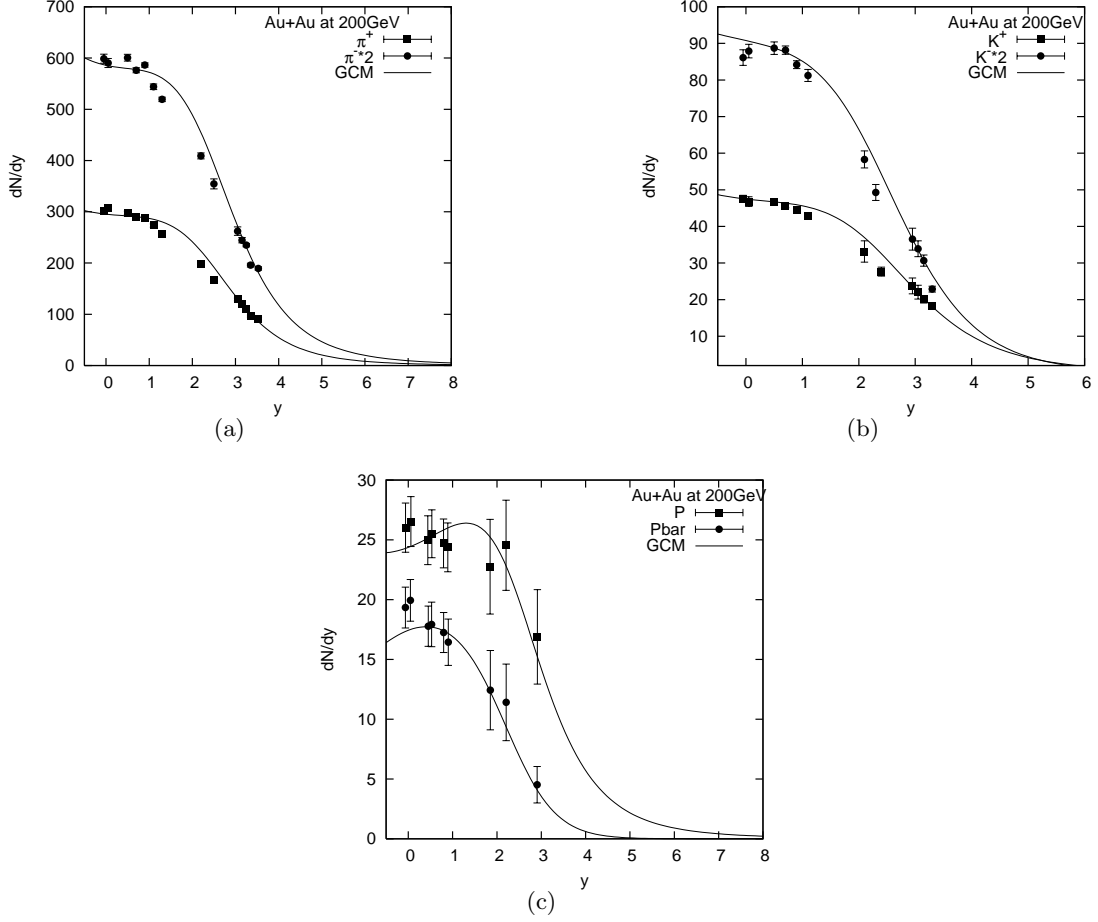


Figure 4: Plot of  $\frac{dN}{dy}$  vs.  $y$  for secondary pion, kaon, proton and antiproton produced in Au+Au interactions at  $\sqrt{S_{NN}} = 200\text{GeV}$  (for  $\beta \neq 0$ ). The different experimental points are from Ref.[22] and the parameter values are taken from Table5. The solid curves provide the GCM-based results.

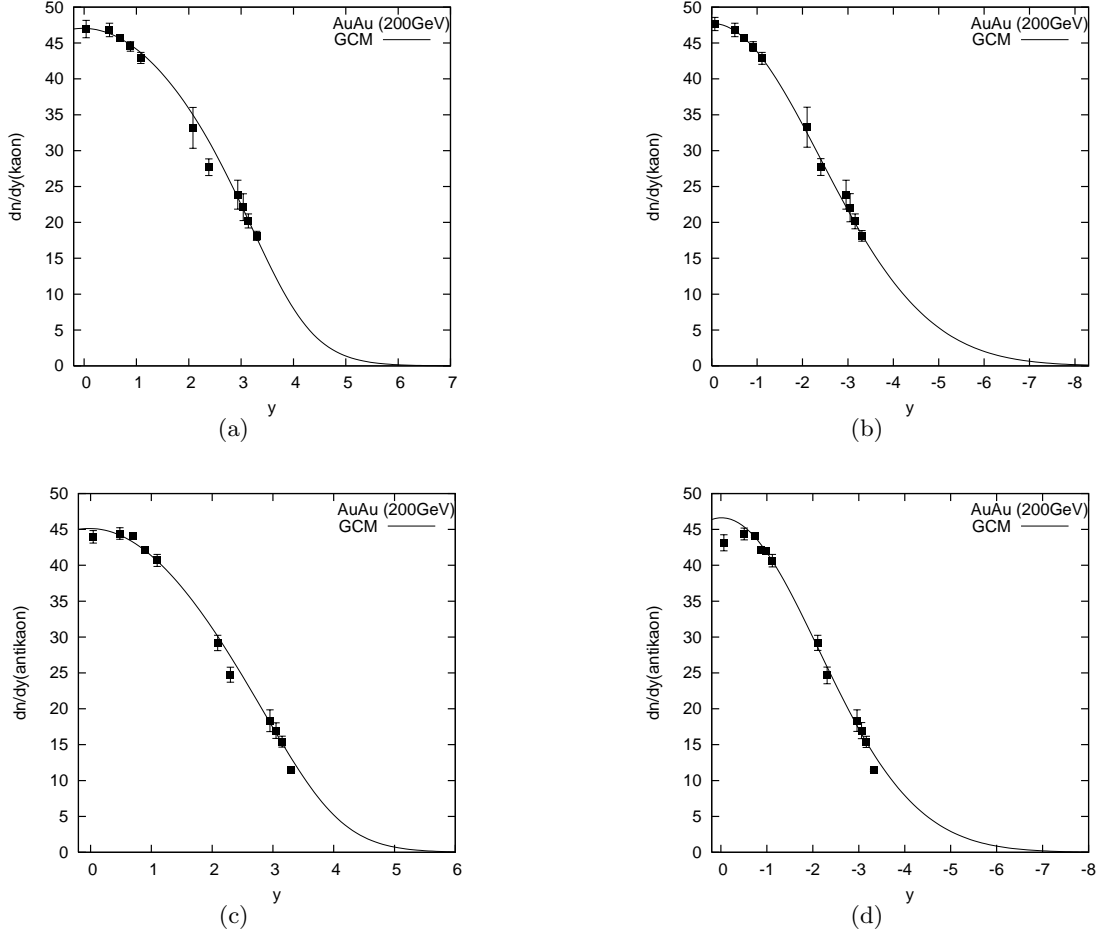


Figure 5: Plot of  $\frac{dN}{dy}$  vs.  $y$  for secondary kaon and antikaon produced in Au+Au interactions for positive and negative  $y$ -values separately at  $\sqrt{S_{NN}} = 200$  GeV (for  $\beta=0$ ), taking  $\Delta=0.55$ . The different experimental points are from Ref.[23] and the parameter values are taken from Table6 and Table7. The solid curves provide the GCM-based results.

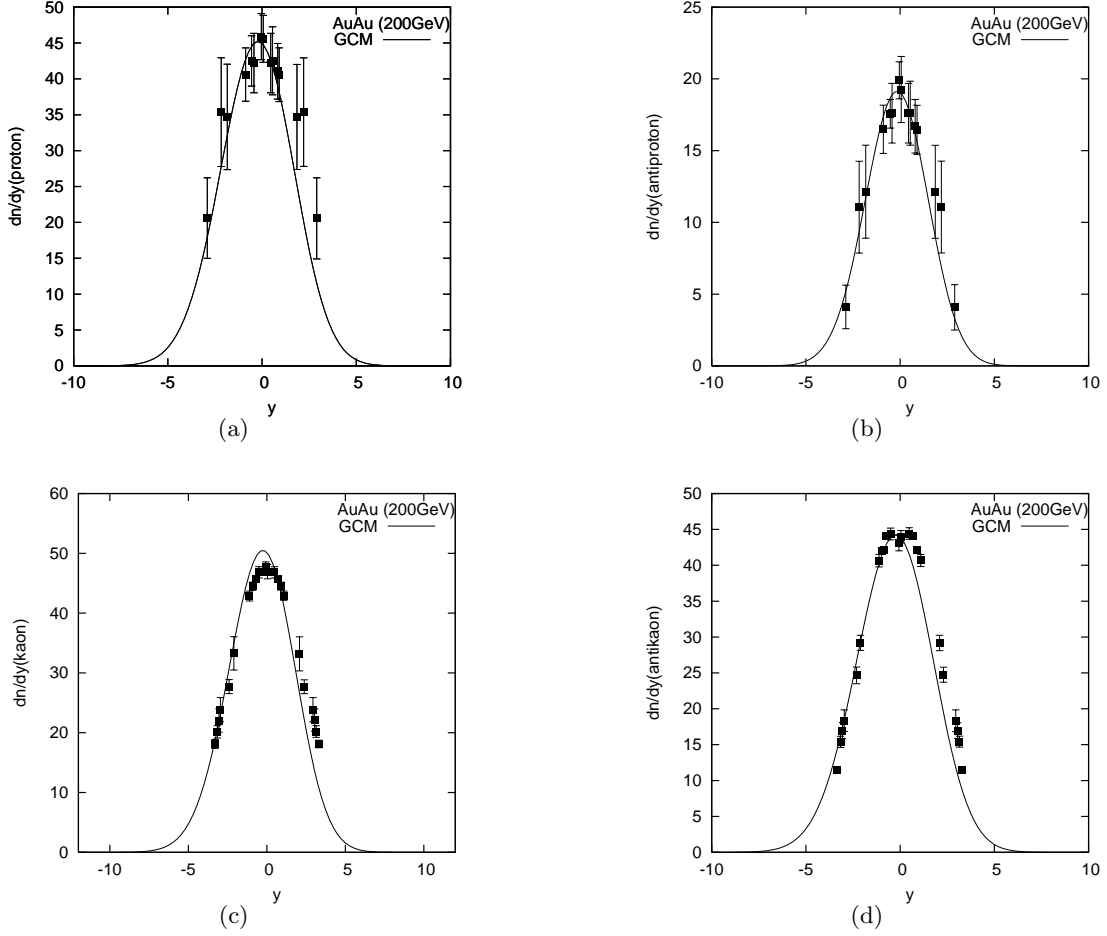


Figure 6: Plot of  $\frac{dN}{dy}$  vs.  $y$  for secondary proton, antiproton, kaon and antikaon produced in Au+Au interactions for positive and negative  $y$ -values separately at  $\sqrt{s_{NN}} = 200$  GeV (for  $\beta=0$ ), taking  $\Delta=1.7$ . The different experimental points are from Ref.[23, 24] and the parameter values are taken from Table 8. The solid curves provide the GCM-based results.

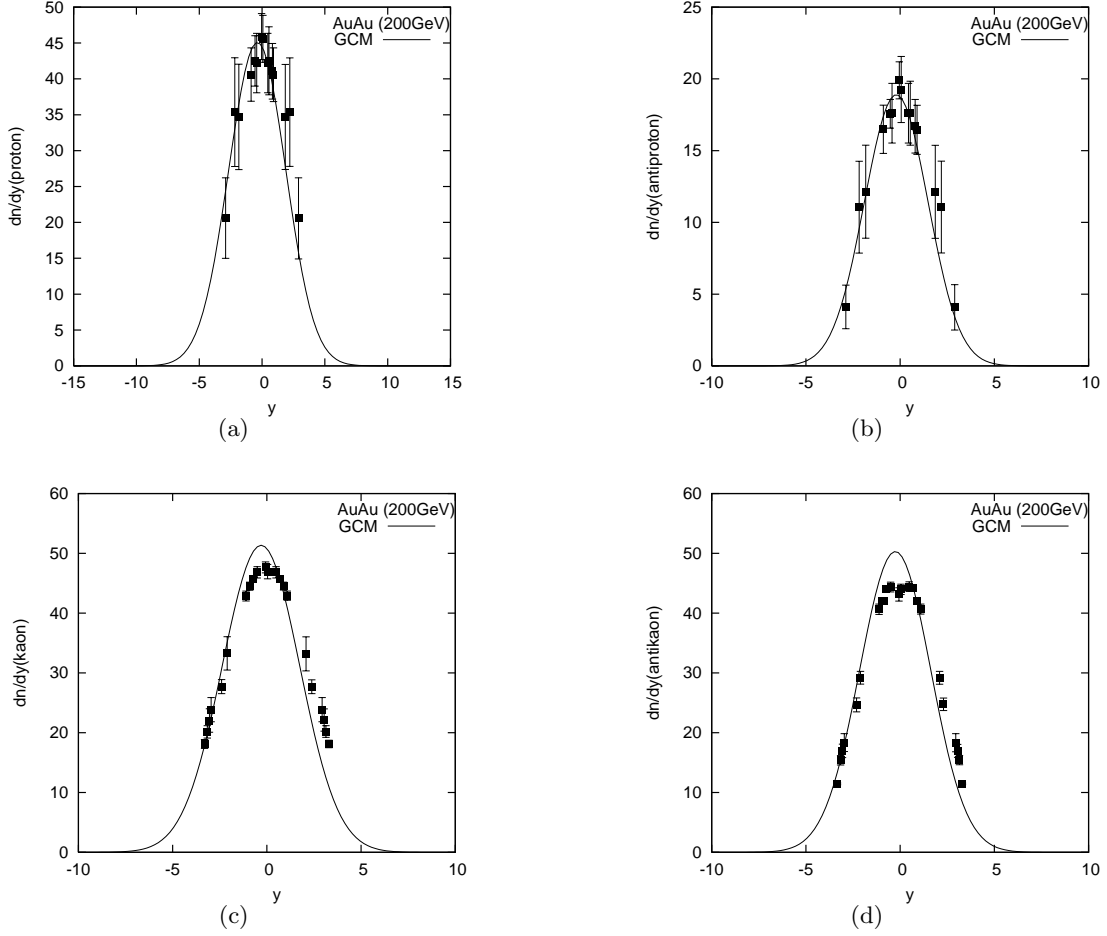


Figure 7: Plot of  $\frac{dN}{dy}$  vs.  $y$  for secondary proton, antiproton, kaon and antikaon produced in Au+Au interactions for positive and negative  $y$ -values separately at  $\sqrt{S_{NN}} = 200$  GeV (for  $\beta=0$ ), taking  $\Delta=3.5$ . The different experimental points are from Ref.[23, 24] and the parameter values are taken from Table9. The solid curves provide the GCM-based results.

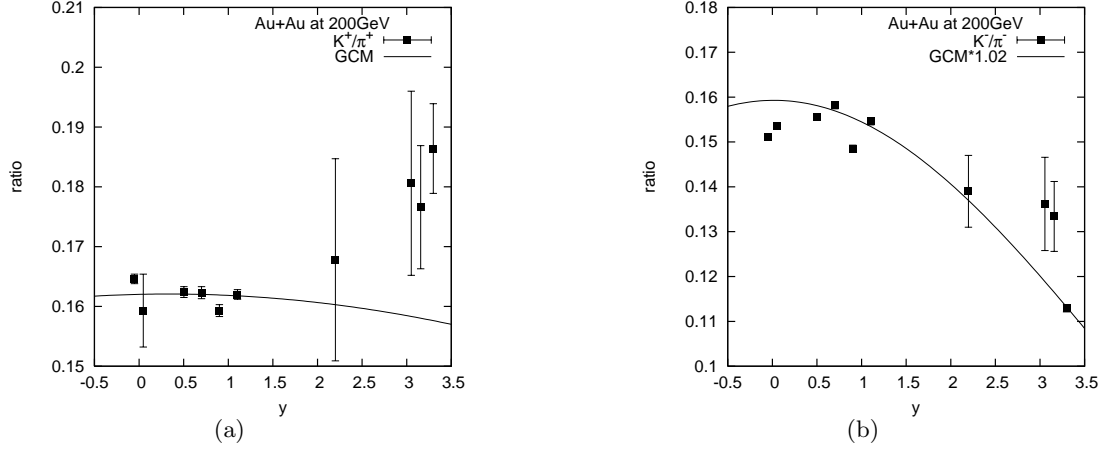


Figure 8: Full phase-space  $K/\pi$  ratios as a function of rapidity systematics at  $\sqrt{S_{NN}} = 200\text{GeV}$ . Errors are statistical only. The different experimental points are from Ref.[25] and the parameter values are taken from Table5. The solid curves provide the GCM-based results.

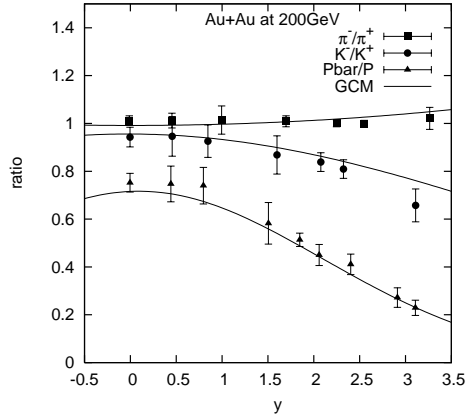


Figure 9: Antiparticle-to-particle ratios as a function of rapidity in central Au+Au collisions at  $\sqrt{S_{NN}} = 200\text{ GeV}$ . The solid lines are our results for  $\pi^-/\pi^+$ ,  $K^-/K^+$ ,  $Pbar/P$  respectively. The experimental data are from Ref.[22] and the parameter values are taken from Table5.

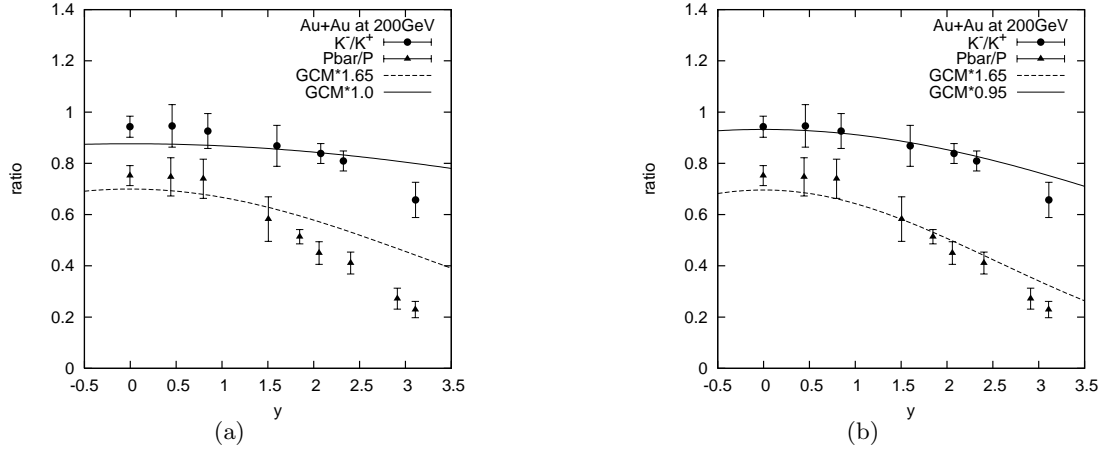


Figure 10: Antiparticle-to-particle ratios as a function of rapidity in central Au+Au collisions at  $\sqrt{s_{NN}} = 200$  GeV. The solid lines are our results for  $K^-/K^+$  and  $Pbar/P$ . The experimental data are from Ref.[22] and the parameter values are taken from Table8 and Table9, taking  $\Delta=1.7$  and  $\Delta=3.5$  for Fig.10(a) and Fig.10(b) respectively.